

**Electron Correlation and the c-axis Dispersion of Cu $d_{3z^2-r^2}$:
a New Band Structure for High Temperature Superconductors**

Jason K. Perry and Jamil Tahir-Kheli

First Principles Research, Inc.

8391 Beverly Blvd., Suite #1711, Los Angeles, CA 90048

www.firstprinciples.com

submitted to *Phys. Rev. Lett.*

Abstract

Previously we showed the major effect of electron correlation in the cuprate superconductors is to lower the energy of the the Cu $d_{x^2-y^2}/O p_\sigma$ ($x^2 - y^2$) band with respect to the Cu $d_{z^2}/O' p_z$ (z^2) band. In our 2D Hubbard model for $\text{La}_{1.85}\text{Sr}_{0.15}\text{CuO}_4$ (LaSCO), the z^2 band is narrow and crosses the standard $x^2 - y^2$ band just below the Fermi level. In this work, we introduce c-axis dispersion to the model and find the z^2 band to have considerable anisotropic 3D character. An additional hole-like surface opens up in the z^2 band at $(0, 0, \frac{2\pi}{c})$ which expands with doping. At sufficient doping levels, a symmetry allowed $x^2 - y^2/z^2$ band crossing along the $(0, 0) - (\pi, \pi)$ direction of the Brillouin zone appears at the Fermi level. At this point, Cooper pairs between the two bands (*e.g.* $(k \uparrow x^2 - y^2, -k \downarrow z^2)$) can form, providing the basis for the Interband Pairing Theory of superconductivity in these materials.

It is generally accepted the proper description of the electronic structure of high temperature superconductors such as $\text{La}_{1.85}\text{Sr}_{0.15}\text{CuO}_4$ (LaSCO) must include electronic correlation beyond that present in LDA band structure computations. Heretofore, it has been implicitly *assumed* the introduction of such correlation would not significantly change the qualitative LDA picture of a broadly dispersing, but very 2D, Cu $d_{x^2-y^2}/\text{O } p_\sigma$ antibonding band ($x^2 - y^2$) as the only band to cross the Fermi level.¹⁻³ Hubbard models developed to study such electron correlation examine the effects of an on-site Coulomb repulsion U on this single $x^2 - y^2$ band, but due to the above assumption, do not consider the effect correlation has on changing the relative position of this band with respect to lower energy fully occupied bands.

We have recently shown that when correlation is introduced in a 2D Hubbard model that explicitly includes Cu $x^2 - y^2$, O p_σ , Cu z^2 , and apical O' p_z orbitals, the band structure is radically altered from LDA results.⁴ We find the overall energy of the $x^2 - y^2$ band is dramatically lowered such that the previously fully occupied Cu $z^2/\text{O}' p_z$ antibonding band (z^2) is also present at the Fermi level rather than several eV lower. This is an intuitively reasonable result given that the $x^2 - y^2$ band is the primary beneficiary of correlation and the principle consequence of correlation is energy stabilization. Thus, the more highly correlated band will be stabilized with respect to the less correlated bands. The effect is so robust that we must conclude any model restricted to just the $x^2 - y^2$ band is doomed to observe only secondary correlation effects while missing completely this primary correlation effect.

In contrast to theories based on a single $x^2 - y^2$ band, the physics arising from this new band structure is straightforward. We calculated that the two bands have a symmetry allowed crossing along the $(0, 0) - (\pi, \pi)$ diagonal of the 2D Brillouin zone very close to the Fermi level. We also showed that, with some empirical adjustments, the crossing could be brought to exactly the Fermi level.⁴ This radically different band structure formed the basis for the Interband Pairing Theory of high temperature superconductivity.⁵ In this theory, phonon coupled Cooper pairs of a completely new form (interband pairs) arise between the two bands in the vicinity of the crossing (*e.g.* $(k x^2 - y^2 \uparrow, -k z^2 \downarrow)$). We demonstrated

that this theory was consistent with the d-wave Josephson tunnelling, the sensitivity of T_c to doping, the Hall effect, the resistivity, and most importantly the NMR, without the need to invoke spin fluctuations or profess the breakdown of Fermi liquid theory.⁵

In this paper, the physical effects of 3D dispersion normal to the CuO_2 planes are incorporated into the original 2D band structure. Such 3D effects are generally not considered in the standard Hubbard models because the $x^2 - y^2$ band, which these models are restricted to, clearly has little 3D dispersion. This is not true of the z^2 band. We find that incorporation of 3D dispersion into this band leads to a critical change in the Fermi surface with the important Fermi level band crossing now arising naturally without the need for any empirical adjustments. This is the main result of this paper.

Additionally, we have shown this new band structure to be consistent with an even wider variety of experimental observations than our previous 2D band structure. These include the angle resolved photoemission (ARPES) single Fermi surface and pseudogap behavior, the mid-IR absorption, the neutron scattering spin incommensurability, the scanning tunneling microscopy (STM) pseudogap, and the X-ray absorption (XAS), while simultaneously improving the quantitative agreement with the LaSCO NMR.⁶

All of these properties stem from symmetry arguments, the rapidly changing orbital character near the Fermi level as the two bands cross, and the Fermi surface that results from the commingling of a 3D band with a 2D band. This is discussed further in the conclusion.

We refined our original LaSCO calculations by obtaining new parameters from a higher level of theory.⁷ Our original parameters were derived from density functional (DFT) BLYP/LACVP*+ calculations on a CuO_6 cluster embedded in a large point charge array. By carefully localizing orbitals we could extract parameters corresponding to orbital energies (E), hopping terms (T), Coulomb energies (U), and exchange energies (K). These terms were then appropriately scaled to account for relaxation effects. Following this same procedure, we have now extracted parameters based on B3LYP/LACV3P*+ calculations. These parameters are reported in Table I.

A complete description of how correlation was introduced to the model is provided

elsewhere.⁴ In essence, under the mean field approximation (which applies in the case of LDA), the Hartree-Fock (HF) orbital energies are determined by

$$E_i = E_i^0 - \sum_j (2 - N_j)(U_{ij} - \frac{1}{2}K_{ij}) \quad (1)$$

where E_i^0 are the calculated orbital energies when all valence bands are full, N_j are the atomic orbital occupations, U_{ij} are the Coulomb terms between orbitals, and K_{ij} are the exchange terms. The correlation problem, which is widely acknowledged to be an important issue in these materials, arises from how the self-Coulomb term is treated. Under the mean field equation, if an orbital is occupied by a single electron, a self-Coulomb term of $U_{ii} - \frac{1}{2}K_{ii} = \frac{1}{2}U_{ii}$ remains. This term comes from repulsion between α and β electrons on the same site. Since spin is expected to be highly polarized, the self-Coulomb term should actually approach zero in the limit of a singly occupied orbital. Thus, to introduce the effect of correlation, we modified the orbital energy equation as follows

$$E_i = E_i^0 - (2 - N_i)U_{ii} - \sum_{j \neq i} (2 - N_j)(U_{ij} - \frac{1}{2}K_{ij}), \quad N_i > 1 \quad (2)$$

$$E_i = E_i^0 - U_{ii} - \sum_{j \neq i} (2 - N_j)(U_{ij} - \frac{1}{2}K_{ij}). \quad N_i \leq 1 \quad (3)$$

Thus, a half-filled band will effectively be lowered in energy by $\frac{1}{2}U_{ii}$ with respect to the fully occupied bands. These equations apply to the orbitals Cu $x^2 - y^2$ and z^2 , and O' p_z . As detailed elsewhere, the O p_σ orbital energies are treated slightly differently since coupling between adjacent Cu sites will reduce the extent of spin polarization on the bridging O.⁴

The 2D band structure that we calculate with the new parameters is presented in Figure 1. The major difference between the original 2D band structure of reference [4] and this new band structure is that the z^2 band is now significantly narrower than before. The existence of a reasonable set of parameters that leads to such a narrow band at the Fermi level is itself a striking result. Qualitatively, the two band structures agree that the broad $x^2 - y^2$ band crosses a narrower z^2 band in the vicinity of the Fermi level. This finding

strongly suggests that this is a robust effect dependent on the introduction of correlation rather than a consequence of parameterization. The dominant effect of changing various parameters appears to be to change the width of the z^2 band, the extent of band repulsion near $(\pi, 0)$, and to a lesser extent the proximity of the band crossing to the Fermi level.

While it is self-evident that the $x^2 - y^2$ band should have very little dispersion along the c -axis and should be very close to a 2D band, the z^2 band has significant apical $O' p_z$ character and should have measurable dispersion along the c -axis. With this in mind, we introduced 3D dispersion in our new Hubbard model by explicitly including the $O' p_z - O' p_z$ hopping term between LaO planes. This hopping term was not calculated like the others. Instead, we chose chemically intuitive values ranging from 0.05 eV to 0.20 eV (this is an order of magnitude smaller than the Cu $d_{x^2-y^2} - O p_\sigma$ coupling). All led to qualitatively the same result, and we ultimately settled on a value of 0.15 eV. The 3D dispersion was further refined by introducing a coupling to effective d_{xz} , d_{yz} , and d_{xy} bands. These bands were taken to lie 2.5 eV above the bottom of the $x^2 - y^2$ band (approximately 0.6 eV below the Fermi level), with xz and yz coupling to the $O' p_z$ orbitals by 0.05 eV and xy coupling by 0.03 eV. This refinement had little effect on the dispersion or the position of the band crossing, but served to remove the 2D Van Hove logarithmic singularities in the density of states. This correction is most important in the computed NMR.⁶

Our 3D band structure is presented in Figure 2. As can be seen, the $x^2 - y^2$ band remains very 2D. In contrast, the z^2 band adopts measurable 3D character. Most significantly, this 3D character is anisotropic. That is, the coupling is maximum at $(0, 0)$ and decreases substantially toward $(\pi, 0)$ and (π, π) . The anisotropy leads to a portion of the z^2 band near $(0, 0, 2\pi/c)$ that lies above the Fermi level. Here, $c = 13.18 \text{ \AA}$ is the height of the doubled unit cell. More importantly, at a particular value of k_z , the $x^2 - y^2/z^2$ band crossing coincides exactly with the Fermi level.

The effect of this modest 3D dispersion on the band structure can be more fully appreciated by consideration of the Fermi surface as presented in Figure 3. From this it becomes clear that a crossing between the two bands is achieved at the Fermi level

along the $(0, 0) - (\pm\pi, \pm\pi)$ symmetry lines. We calculate this to occur in the vicinity of $k_z = 1.54\pi/c$ at optimal doping. No empirical adjustments were necessary beyond that described above. This new Fermi surface is basically 2D in nature when underdoped, but upon doping, electrons are removed near $(0, 0, 2\pi/c)$. This new 3D hole-like surface expands until it reaches the 2D Fermi surface along the diagonal. At that point electrons are removed from a second band in the vicinity of the crossing. The Fermi surface crossing originates at $k_z = 2\pi/c$, but as doping continues, the crossing occurs at lower values of k_z .

What is striking about this new band structure is that a symmetry allowed band crossing occurs exactly at the Fermi level. While band crossings occur all the time, the probability of a band crossing at the Fermi level is extremely small. However, the cuprates are distinguished from ordinary metals in the ease with which they may be doped. This allows the system to be tuned to exactly the dopings that have a band crossing at the Fermi level. We believe this is the reason for the strong T_c dependence of the cuprates to doping.

When such a crossing occurs at the Fermi level, Cooper pairs ($k \uparrow$ from one band and $-k \downarrow$ from the other band) can form in the vicinity of the crossing. Such pairs are not time-reversal invariant with themselves and lead to a simple explanation for the d-wave Josephson tunneling with coupling due to phonons.^{5,8} A computation of the dielectric function that arises from this band structure shows the electron gas is unable to adequately screen the electron-phonon attractive coupling leading to a possible explanation for why T_c is so high.⁸

The band structure is equally successful in explaining a diverse spectrum of high T_c normal state properties. Most of the unusual phenomena associated with these materials derives from the fact that in the vicinity of a band crossing, the orbital character of the two bands is changing very rapidly. It is no longer correct to assume the density of states is approximately constant over the energy range plus/minus a few kT when performing standard band theory integrals. Thus, in the computation of the NMR for example, the bare densities of states for $x^2 - y^2$, z^2 , and p_σ are strongly dependent on energy and cannot be taken out of the integral.⁶ One can also see that such a crossing at the Fermi level will

lead to a rapid change in the curvature of the constant energy surfaces in the vicinity of the Fermi level and hence a large temperature variation in the Hall effect.⁵

Furthermore, there will be optical absorption down to zero energy at the band crossing point. Along the line $(\pi, 0) - (\pi, \pi)$, the bands must repel and the minimum separation of the two bands (≈ 0.1 eV) will lead to a peak in the mid-IR absorption as is observed.⁶ Additionally, the large ARPES background arises naturally due to inelastic scattering of z^2 electrons near the Fermi energy.⁶ In fact, the inability of ARPES to fully resolve the z^2 band due to its strong k_z dependence can lead to a “d-wave” pseudogap, which is simply a measure of the size of the $x^2 - y^2/z^2$ band repulsion at each k value.

An important unresolved issue with our band structure is the semiconducting c-axis resistivity.⁹ Since the density of states of the z^2 band is large and varying rapidly with energy, the number of charge carriers in each band will change as the temperature is raised. As k states with mostly $x^2 - y^2$ character have essentially no dispersion normal to the planes and k states with predominantly z^2 character disperse strongly in this direction, the possibility exists that a semiconducting resistivity may arise. Such a computation is presently being done including the expected temperature variation of the scattering rates of the two bands to determine if this is the case.

While we advocate this new band structure based on *ab initio* grounds, our strongest arguments in favor of this picture come from what can be explained and what can be calculated using standard equations from band theory. We believe the above success of this new cuprate band structure is a strong argument in its favor.

References

- [1] W.E. Pickett, Rev. Mod. Phys. **61**, 433 (1989); J. Yu, A.J. Freeman, and J.H. Xu, Phys. Rev. Lett. **58**, 1035 (1987); L.F. Mattheiss, Phys. Rev. Lett. **58**, 1028 (1987).
- [2] P.W. Anderson “The Theory of Superconductivity in the High- T_c Cuprates,” (Princeton University Press, Princeton, NJ; 1997); D.J. Scalapino, *Phys. Rep* **250**, 330 (1995).

- [3] M.S. Hybertsen, E.B. Stechel, W.M.C. Foulkes, and M. Schlüter, Phys. Rev. B **45**, 10032 (1992).
- [4] J.K. Perry and J. Tahir-Kheli, Phys. Rev. B **58**, 12323 (1998); J.K. Perry, J. Phys. Chem., in press (xxx.lanl.gov/cond-mat/9903088).
- [5] J. Tahir-Kheli, Phys. Rev. B **58**, 12303 (1998).
- [6] J. Tahir-Kheli, J. Phys. Chem., in press (xxx.lanl.gov/cond-mat/9903105); J.K. Perry and J. Tahir-Kheli, Phys. Rev. Lett., submitted (xxx.lanl.gov/cond-mat/9908308); J. Tahir-Kheli and J.K. Perry, to be published.
- [7] Parameters were obtained from Jaguar 3.5, Schrödinger, Inc., Portland, OR.
- [8] J. Tahir-Kheli, to be submitted.
- [9] S.L. Cooper and K.E. Gray, *Physical Properties of High Temperature Superconductors* vol 3, p 61-188, edited by D.M. Ginsberg, World Scientific, 1990.

Table I. Hubbard parameters for 3D band structure (in eV). E is an orbital energy for optimal doping, E^0 is an orbital energy when all bands are full, T an orbital coupling matrix element, U a Coulomb repulsion term, and K an exchange energy term. c-axis coupling terms provided in text.

$E(x^2 - y^2)$	-3.085	$E^0(x^2 - y^2)$	-2.77	$U(x^2 - y^2/x^2 - y^2)$	14.95
$E(z^2)$	-1.011	$E^0(z^2)$	-2.90	$U(z^2/z^2)$	10.42
$E(O p_\sigma)$	-4.143	$E^0(O p_\sigma)$	-9.46	$U(O p_\sigma/O p_\sigma)$	13.74
$E(O' p_z)$	-3.717	$E^0(O' p_z)$	-10.30	$U(O' p_z/O' p_z)$	6.13
		$U(x^2 - y^2/z^2)$	11.48	$K(x^2 - y^2/z^2)$	1.06
$T(x^2 - y^2/O p_\sigma)$	1.56	$U(x^2 - y^2/O p_\sigma)$	5.05	$K(x^2 - y^2/O p_\sigma)$	0.10
		$U(x^2 - y^2/O' p_z)$	3.86	$K(x^2 - y^2/O' p_z)$	0.03
$T(z^2/O p_\sigma)$	0.15	$U(z^2/O p_\sigma)$	4.54	$K(z^2/O p_\sigma)$	0.07
$T(z^2/O' p_z)$	1.50	$U(z^2/O' p_z)$	4.46	$K(z^2/O' p_z)$	0.90
$T(O p_\sigma/O p'_\sigma)$	0.59	$U(O p_\sigma/O p'_\sigma)$	4.31	$K(O p_\sigma/O p'_\sigma)$	0.06
$T(O p_\sigma/O p''_\sigma)$	0.14	$U(O p_\sigma/O p''_\sigma)$	3.36	$K(O p_\sigma/O p''_\sigma)$	0.08
$T(O p_\sigma/O' p_z)$	-0.27	$U(O p_\sigma/O' p_z)$	3.85	$K(O p_\sigma/O' p_z)$	0.11
$T(O' p_z/O' p'_z)$	0.94	$U(O' p_z/O' p'_z)$	3.63	$K(O' p_z/O' p'_z)$	0.53

Figure Captions

Figure 1. Calculated 2D band structure a) without correlation and b) with correlation. The energy of the $x^2 - y^2$ band is stabilized with respect to the z^2 band with the inclusion of correlation.

Figure 2. Calculated 3D band structure. The $x^2 - y^2$ band remains very 2D, but the z^2 band adopts measurable anisotropic 3D dispersion. Near $(0, 0, 2\pi/c)$, the z^2 band lies above the Fermi level.

Figure 3. Calculated 3D Fermi surface. Cross sections shown at $k_z = 2\pi/c$, $k_z = 1.54\pi/c$, $k_z = 1.30\pi/c$, and $k_z = 0$.

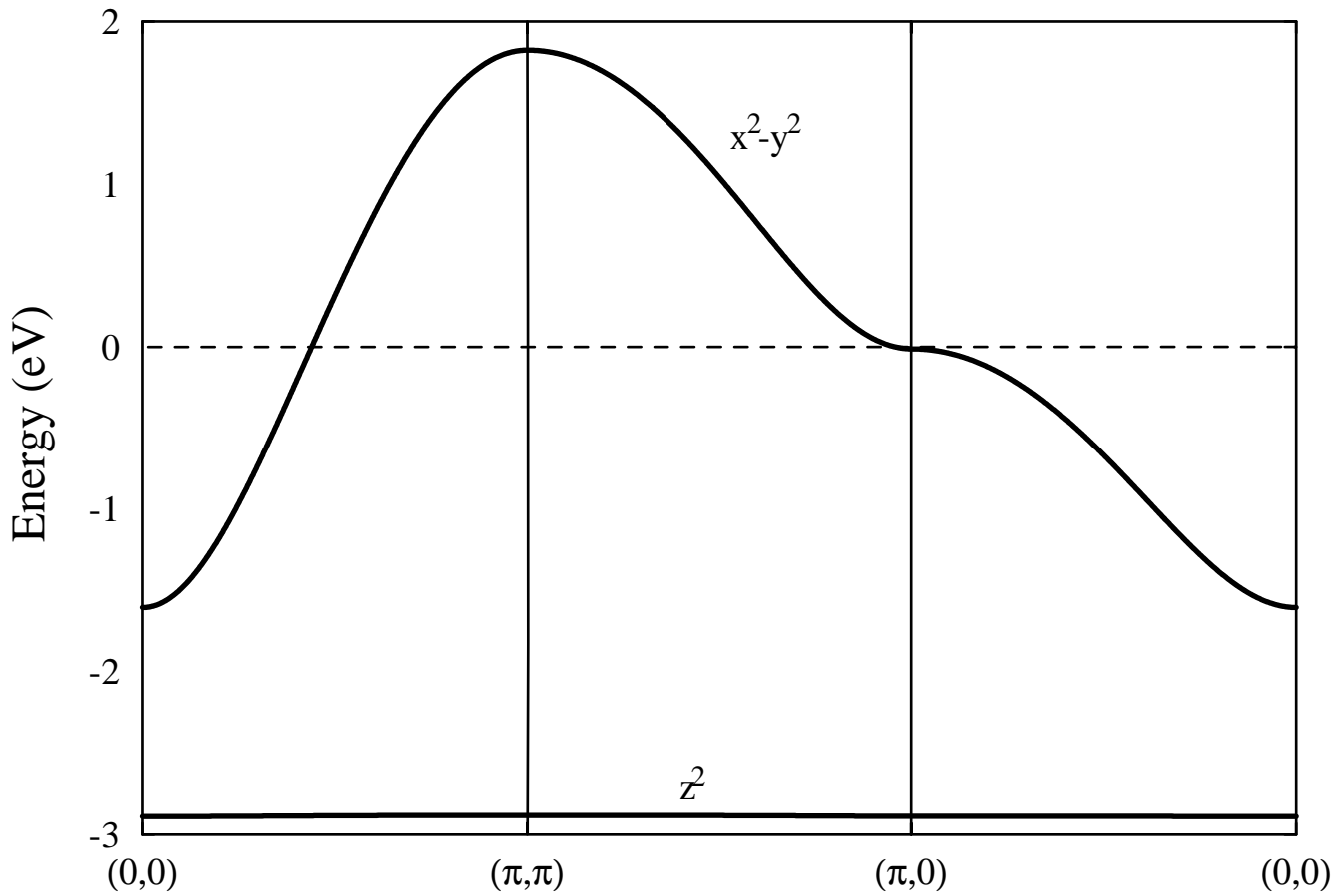


Figure 1a.

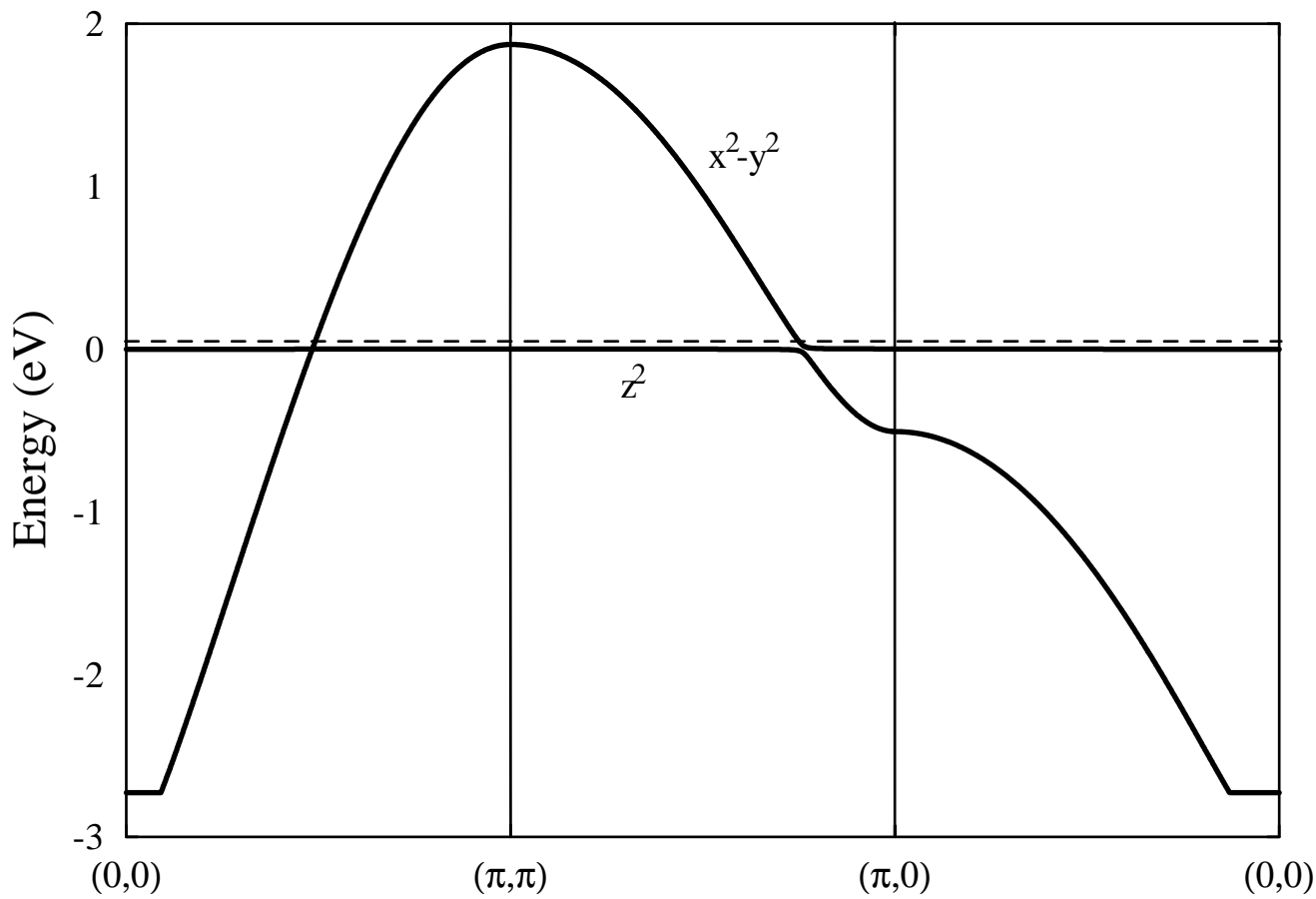


Figure 1b.

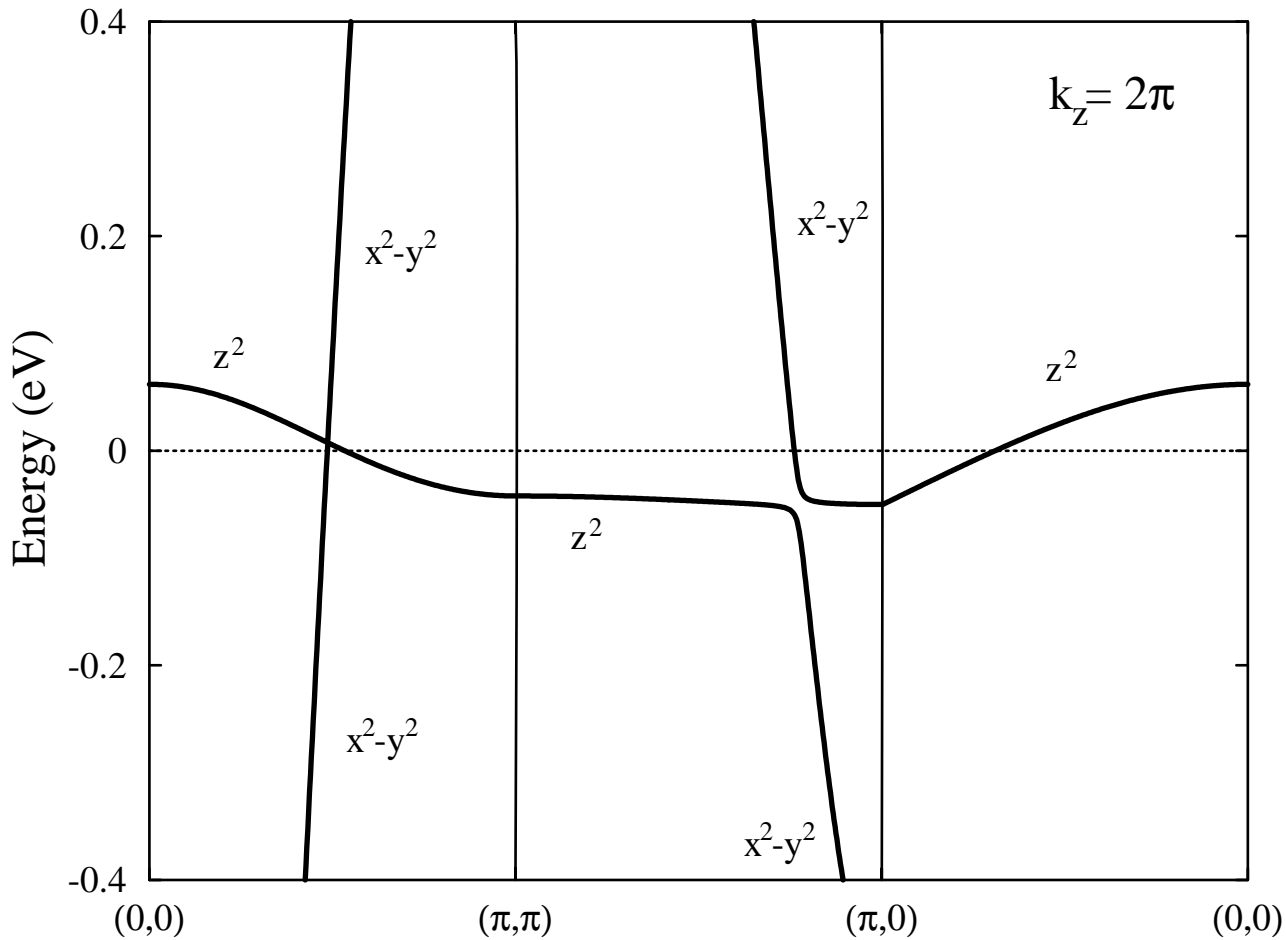


Figure 2a.

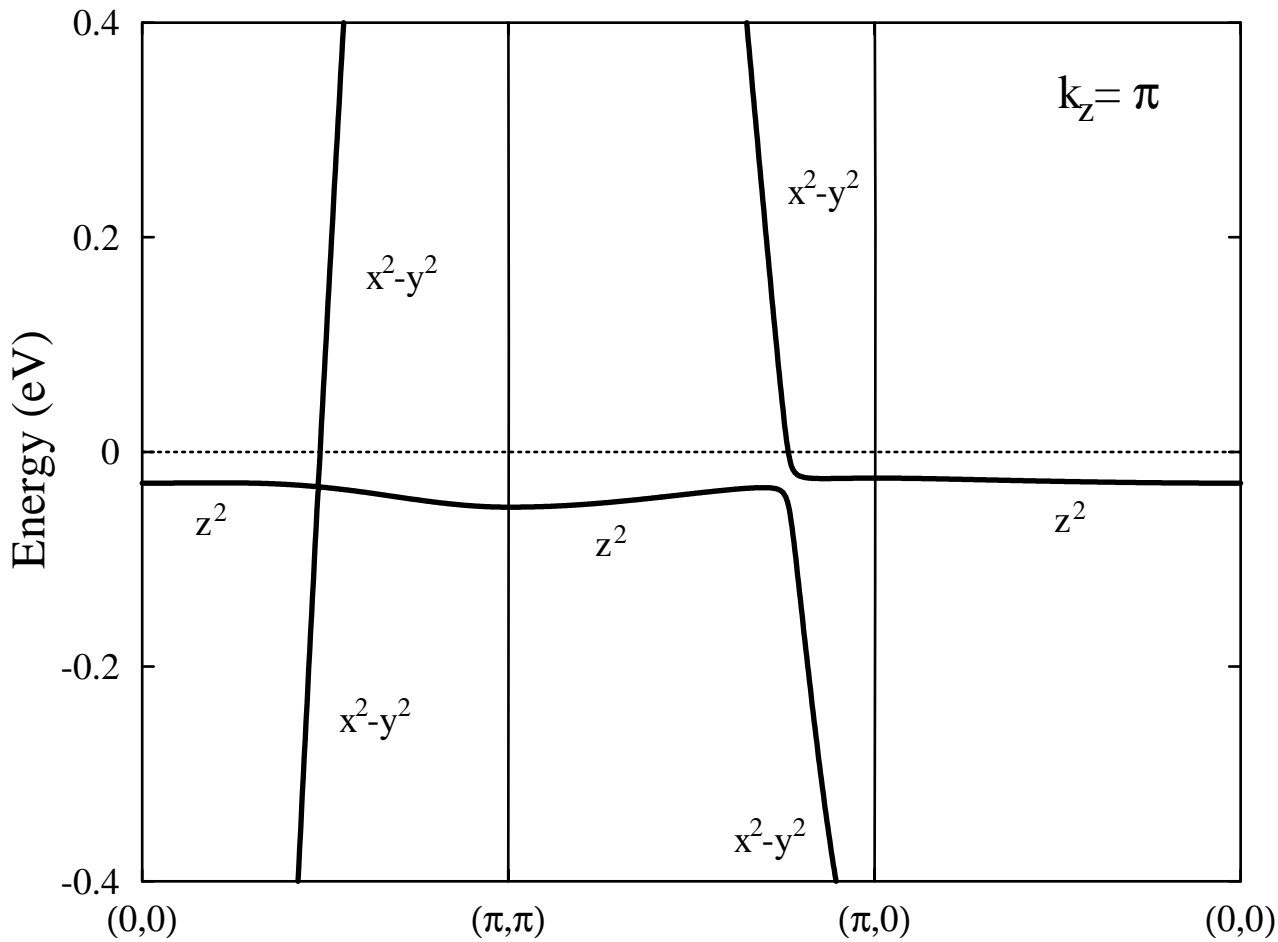


Figure 2b.

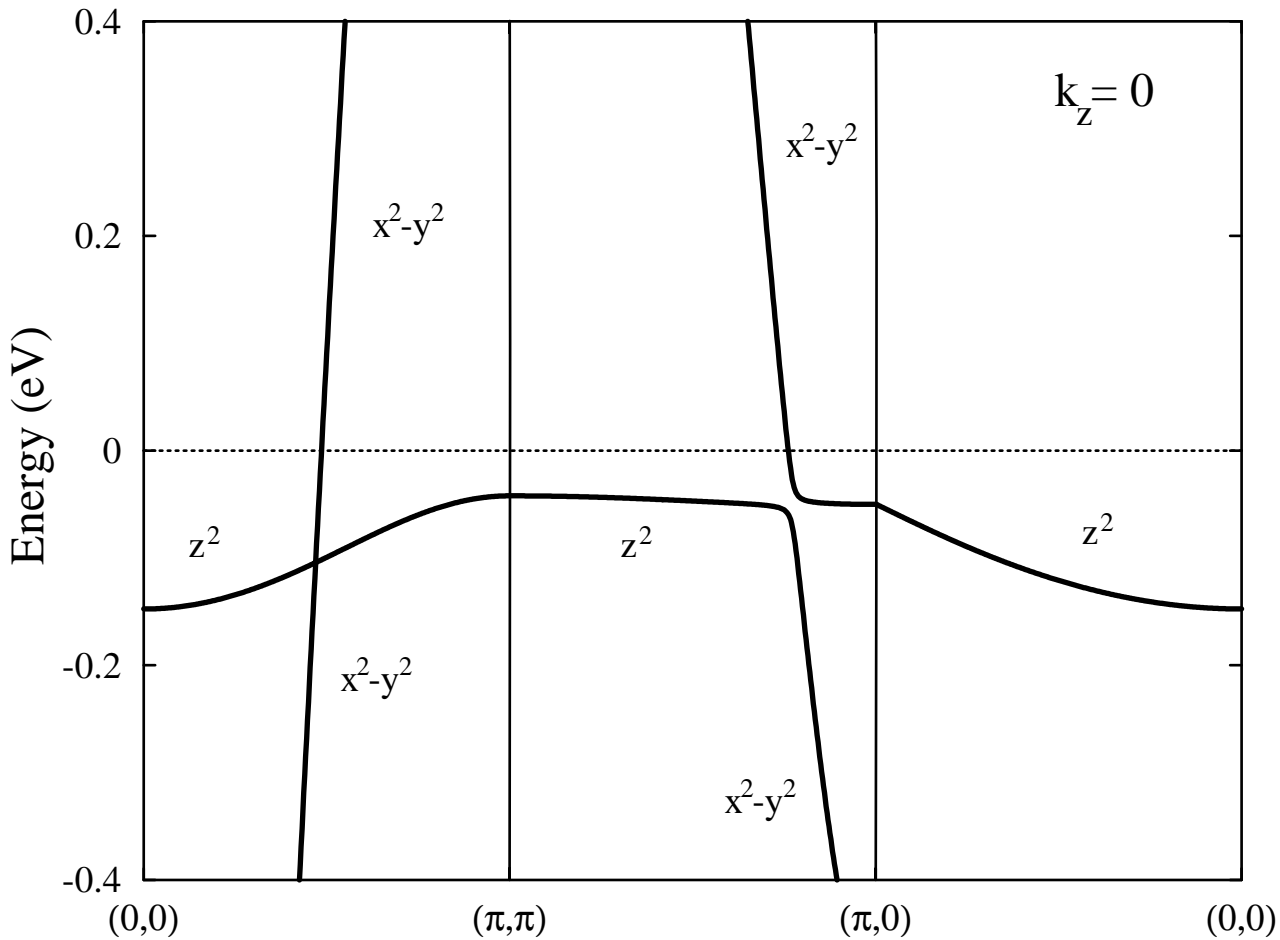


Figure 2c.

Figure 3

